

# Anomalous reflection coefficient underlying experimentally validated outstanding transmission through metal–dielectric–metal microcavities

Alejandro Doval , Lucía Suárez-Fernández , Raúl de la Fuente , and Yago Arosa\* 

Instituto de materiais da USC - iMATUS, Grupo de Nanomateriais, Fotónica e Materia Branda, Departamento de Física Aplicada, Universidade de Santiago de Compostela, E-15782, Santiago de Compostela, Spain

Received 27 October 2025 / Accepted 29 December 2025

**Abstract.** Analytical modelling of light transmission through a metal-insulator-metal geometry embedded in a coupling glass surrounding medium is possible through an extended Fabry-Pérot formula. Two distinct coupled surface plasmon resonance branches are allowed inside such microcavity, where two thin metallic layers act as mirrors delimiting an inner dielectric material. In agreement with transfer-matrix method simulations, the resulting theoretical expressions predict a large and almost constant transmittance even for intracavity thicknesses greater than light's penetration depth. Results at  $\lambda = 800$  nm have been validated experimentally and show optical transmittance over 10% until nearly 3  $\mu\text{m}$ . This high transmittance under such unexpected conditions, related to an anomalously high mirror reflection coefficient, sheds light on new possibilities for the design of optical devices. The experimental setup successfully used to corroborate the validity of the transmittance formula over different angular, spectral and geometrical conditions is also presented.

**Keywords:** Plasmonics, Coupled surface plasmons, Microcavities, Transmittance, Resonance.

## 1 Introduction

Coupled Surface Plasmons (CSP) in metal-dielectric-metal (MDM) and dielectric-metal-dielectric (DMD) geometries started attracting theoretical interest since the late 20th century [1]. Initial experimental validations [2] opened the path for posterior applications of both arrangements. Specifically, referring to the case of MDM geometry that we will be addressing in this work, applications range from guiding systems [3] to spectral filtering [4], including sensors [5] or spectroscopy [6] as well.

Our recent studies [7] have focused on developing and validating an analytical model for transverse magnetic (TM)-polarized light transmission through an optical plasmonic microcavity (MC), involving an MDM structure. The MC is formed by two thin plane metallic mirrors (M) separated by a low-index dielectric gap (L) and surrounded by two semi-infinite higher-index dielectric media (H). An analytical expression for  $T$  – see equation (1) – was obtained by application of Fresnel coefficients at the interfaces, and the subsequent results were calculated by implementing Fresnel formalism for coherent optical scattering at an interface and validated by comparison with simulations

using in-house developed software based on transfer-matrix-method [8]. Experimental validation was also carried out, using two identical symmetrically arranged prisms playing the role of the external semi-infinite high-index media, which couple and decouple light to the possible plasmonic resonances of the inner structure.

$$T = \frac{|t_{\text{LMH}}|^2 |t_{\text{HML}}|^2}{4|r_{\text{LMH}}|^2 \left[ \sinh^2(k''_{L,\perp} d - \ln|r_{\text{LMH}}|) + \sin^2(k'_{L,\perp} d + \varphi_{\text{LMH}}) \right]} \quad (1)$$

where  $r_{\text{LMH}}$  and  $t_{\text{LMH}}$  are reflection and transmission field amplitude coefficients for each of the two three-medium mirror structures;  $\varphi_{\text{LMH}}$  represents the phase of  $r_{\text{LMH}}$ ;  $d$  denotes the intracavity thickness; and  $k_{L,\perp} = k'_{L,\perp} + ik''_{L,\perp}$  is the component of the intracavity wavevector in the direction perpendicular to the interfaces. This equation can be seen as a generalization of the common formula for transmittance in Fabry-Pérot (FP) interferometers to all incidence angles, from which the different resonant modes in the system can be obtained. On the one hand,  $k_{L,\perp}$  is real for incidence angles  $\theta$  below the critical angle for incidence from H to L,  $\theta_{\text{cr}}$ , for which volume resonances are allowed. That case corresponds to the well-known FP regime, in which harmonic waves can

\* Corresponding author. [yago.arosa.lobato@usc.es](mailto:yago.arosa.lobato@usc.es)

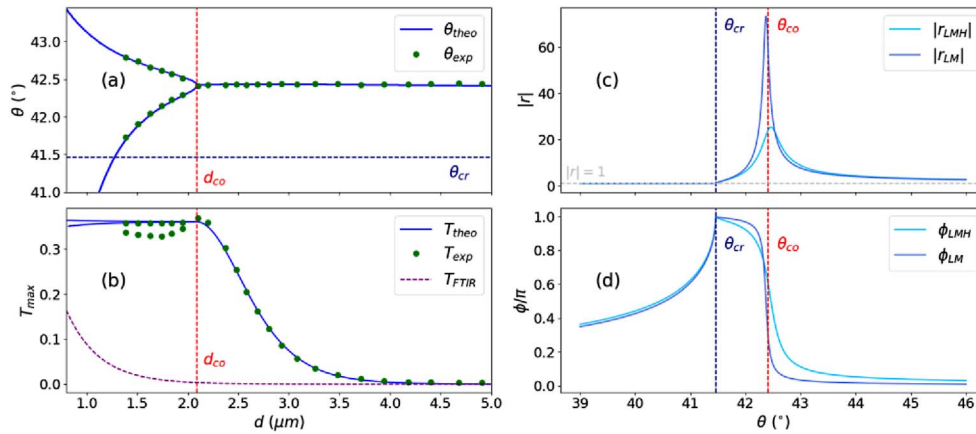


**Fig. 1.** (a) Angle of incidence at which the transmittance of each CSP is maximum as a function of cavity thickness. (b) Maximum transmittance at each CSP resonance peak as a function of cavity thickness, FTIR transmission at  $\theta_{co}$  without Ag for comparison. (c) Modulus and (d) phase of  $r_{LMH}$  (lighter) and  $r_{LM}$  (darker) as functions of the incident angle. All results correspond to a setup using silver as metal ( $d_M = 39$  nm), BK7 as prism and air filling the gap between the mirrors, at  $\lambda = 800$  nm.

propagate between the two mirrors at photonic resonance conditions. On the other hand, for  $\theta > \theta_{cr}$ ,  $k_{L,\perp}$  becomes imaginary, and only CSP resonances are allowed. In both cases, the dependence on the separation between the mirrors,  $d$ , in equation (1) becomes straightforward, since it only appears inside the argument of either the sine or the hyperbolic sine, respectively. As a result, CSP resonances correspond to zeros of the hyperbolic sine, leading to two distinct solutions for each  $d$  at two different  $\theta$ , as shown in Figure 1a. It is also remarkable that one of these two curves is the continuation of the first FP resonance, forming a hybrid branch. For thick enough cavities these two plasmonic resonances become degenerated, merging at the same angular position – named the coalescence angle  $\theta_{co}$  – for  $d > d_{co} = \max[(\ln|r_{LMH}|)/k'_{L,\perp}]$ .

In this work, we emphasize the high values of transmittance in the system even for over-wavelength-thick cavities. The presented theoretical and experimental studies of maximum transmittance as a function of  $d$  reveal that it remains not only noticeable but also large for  $d$  exceeding by far the predicted penetration depth of light in the intracavity  $L$  medium. Thus, transmittance of CSP resonances in this MC can be said to resemble some kind of enhanced light tunneling. Analysis of equation (1) reveals that  $r_{LMH}$  is the key parameter determining this phenomenon, especially in the plasmonic regime. A brief theoretical analysis on the behavior of that reflection coefficient is also presented. Its modulus becomes much larger than unity near the coalescence. This may seem surprising if one thinks of Fresnel coefficients as the square root of reflectance ( $R$ ). However, there is no issue with energy conservation here because the waves involved are evanescent and  $|r| = \sqrt{R}$  does not hold.

## 2 Material and methods

The experimental setup used to test our theoretical predictions is shown in Figure 2. A supercontinuum light source

(SuperK COMPACT, NKT Photonics, 450–2400 nm) illuminates the MC, with power adjusted by a variable neutral optical density. A cube polarizer provides a transmitted TM beam, which is a requirement for the excitation of surface plasmons. Simultaneously, part of the original beam is deflected towards a photodiode, used to monitor the beam power. The MC consists of two identical rectangular BK7 glass coupling prisms, whose largest faces are coated with thin silver films, facing each other and creating a micron-scale air gap in between. That cavity thickness is determined by iteratively comparing with subsequent theoretical configurations, varying  $d$  with the desired precision. It is modified in  $\sim 20$  nm steps using a piezoelectric actuator (Thorlabs PIAK25), which is connected to the prisms through custom 3D-printed mounts. These are mounted on a rotation platform (URS75BCC from Newport Optics), that allows us to control the angle of incidence ( $\pm 6$  mdeg accuracy). Finally, the transmitted signal is collected with a photodiode preceded by a spectral filter, enabling monochromatic mapping of  $T$  across a 2D  $\theta - d$  space, using incident light as a reference.

The thin silver layers on the prisms, used as MC mirrors, were deposited by physical vapor deposition (PVD), evaporating the metal through heating. The prisms were placed inside the vacuum chamber of a Baltec BAE250 Coating System by Balzers, and the pressure was reduced to  $\sim 10^{-3}$  Pa. Afterwards, the silver was heated until it started to evaporate ( $\sim 140$  °C), and an approximately constant deposition rate was used to obtain silver films with a nominal thickness around 39 nm. Later, this value was found to be correct within an uncertainty range of  $\pm 5$  nm with a Dektak3 Surface Profilometer, as an extra check.

## 3 Results and discussion

The analytical model developed for transmittance of the MC was experimentally validated. Angular positions of

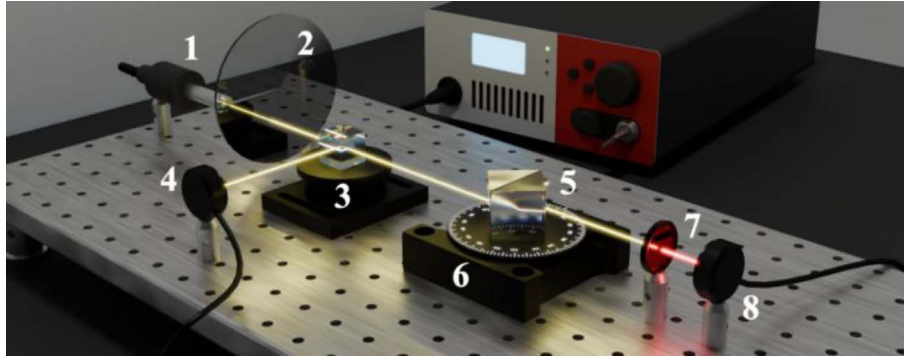


**Fig. 2.** 3D schematic drawing of the experimental setup. (1) Output of the supercontinuum light source, (2) variable optical density filter, (3) cube acting as polarizer and beam splitter, (4) power monitoring photodiode, (5) couple of prisms conforming the MC, (6) rotation platform, (7) narrowband spectral filter, (8) photodiode detector for measuring transmittance.

the transmittance maxima for the two CSP resonances as a function of  $d$  at a fixed wavelength  $\lambda = 800$  nm are displayed in Figure 1a, while their peak values are presented in Figure 1b. Both graphs show the agreement between theoretical predictions and experimental measurements. Those results correspond to a BK7-Silver-Air MC, with metallic mirror thickness  $d_M = 39$  nm. Peak values for transmittance remain high and almost constant until the coalescence thickness, which is well beyond the wavelength (in this case,  $d_{co} = 2.1$   $\mu\text{m}$ ). Besides, the maximum observed transmittance decreases slowly for  $d > d_{co}$ , staying above 10% until  $d = 2.9$   $\mu\text{m}$ , exceeding by far the theoretical penetration depth of light into the air gap, calculated to be  $\delta = [k_{L\perp}''(\theta_{co})]^{-1} \approx 652$  nm in this situation, with  $\theta_{co} \approx 42.4^\circ$ .

The resonance conditions derived from equation (1) are clearly highly dependent on  $r_{LMH}$ , whose modulus and phase appear in the arguments of the hyperbolic sine and sine, respectively (with the former determining CSP resonances and the latter defining FP resonances). This three-layer reflection coefficient can be expressed in terms of Fresnel coefficients  $r_{ML}$ ,  $r_{MH}$ :

$$r_{LMH} = \frac{-r_{ML} + r_{MH} e^{i\phi_M}}{1 - r_{ML} r_{MH} e^{i\phi_M}} \quad \text{with} \quad (2)$$

$$\phi_M = 2 d_M \cdot k_{M\perp} = 2 d_M \cdot k_0 \sqrt{\varepsilon_M - \varepsilon_H \sin^2 \theta},$$

where  $\varepsilon_i$  stands for the permittivity of medium  $i$  and  $k_{M\perp}$  denotes the component of the wavevector inside the metal normal to the interfaces. The modulus and phase of  $r_{LMH}$  are plotted in Figure 2c and 2d as functions of the incident angle  $\theta$ , together with those for Fresnel coefficient  $r_{LM}$ , corresponding to the limiting case where the delimiting metallic mirrors are semi-infinite ( $d_M \rightarrow \infty$ ). The modulus  $|r_{LMH}|$  is seen to behave differently below and above  $\theta_{cr}$ . When harmonic propagation inside the cavity is allowed, it stays slightly below 1. In turn, it grows far greater than 1 above  $\theta_{cr}$ , reaching its maximum value around  $\theta_{co}$ . Separation from  $\theta_{co}$  is due to the role played by the rest of the argument of the hyperbolic sine in equation (1). The thicker the metallic mirrors, the higher the peak in  $|r_{LMH}|$ , converging to  $|r_{LM}|$  for large  $d_M$ . For  $\theta > \theta_{cr}$ ,

$|r_{LMH}|$  and  $|r_{LM}|$  being greater than 1 means no problem in terms of energy conservation, since the amplitudes related by them correspond to the electric fields of evanescent waves [9]. Focusing on the phase, it grows gradually for  $\theta < \theta_{cr}$ , reaching  $\pi$  at  $\theta = \theta_{cr}$ . For larger angles, it starts decreasing slowly until  $\theta$  approaches  $\theta_{co}$ , when it suddenly drops to nearly zero, undergoing a slow decline again at the end. Finally, comparison with  $r_{LM}$  reveals that the drop is steeper for larger  $d_M$ . This anomalous behavior of  $r_{LMH}$  above  $\theta_{cr}$  – large modulus and step-like phase – happens especially at the same angles  $\theta \approx \theta_{co}$  at which outstanding transmittance occurs.

## 4 Conclusions

The experimentally validated analytical formula for T through an MDM structure predicts high and constant transmittance for cavity thicknesses far above the penetration depth of light. This outstanding transmittance is key for the use of CSP-based arrangement in devices for different applications. These include sensing thin media, for which measurements based on light transmission instead of reflection can simplify experimental setups; highly selective optical filtering, spectroscopy or light control at the nanoscale.

## Funding

This research was funded through projects by the Spanish Ministry of Science, Innovation and Universities (PID2024-156552OA-I00), Universidade de Santiago de Compostela (USC 2024-PU031) and Xunta de Galicia (GRC ED431C 2024/06), respectively. Finally, AD thanks the Spanish Ministry of Science, Innovation and Universities for the financial support through FPU21/01302, as well as YA acknowledges Xunta de Galicia for the postdoctoral fellowship ED481D-2024-001.

## Conflicts of interest

The authors have nothing to disclose. They certify that they have no financial conflicts of interest (e.g., consultancies, stock ownership, equity interest, patent/licensing arrangements, etc.) in connection with this article.

**Data availability statement**

Data associated with this article is available under request.

**Author contribution statement**

Conceptualization, R.F.; Methodology, Y.A.; Software, A.D., Y.A.; Validation, A.D.; Formal Analysis, R.F.; Investigation, A.D., Y.A., L.S., R.F.; Data Curation, Y.A., L.S.; Writing – Original Draft Preparation, A.D.; Writing – Review & Editing, R.F., Y.A.; Visualization, Y.A., A.D.; Supervision, R.F.; Project Administration & Funding Acquisition, Y.A., R.F.

**References**

- 1 Economou EN, Surface plasmons in thin films, *Phys. Rev.* 182, 2 (1969). <https://doi.org/10.1103/PhysRev.182.539>.
- 2 Welford KR, Sambles JR, Coupled surface plasmons in a symmetric system, *J. Mod. Opt.* **35**, 9 (1988). <https://doi.org/10.1080/09500348814551611>.
- 3 Marquis CD et al., Excitation of “forbidden” guided-wave plasmon polariton modes via direct reflectance using a low refractive index polymer coupling layer, *PLoS One* **17**, 10 (2022). <https://doi.org/10.1371/journal.pone.0276522>.
- 4 Yoon YT, Lee SS, Transmission type color filter incorporating a silver film based etalon, *Opt. Exp.* 18, 5 (2010). <https://doi.org/10.1364/OE.18.005344>.
- 5 Huang BR et al., Reduction of angular dip width of surface plasmon resonance sensor by coupling surface plasma waves on sensing surface and inside metal–dielectric–metal structure, *J. Vacuum Sci. Technol. A* 31, 6 (2013). <https://doi.org/10.1116/1.4821505>.
- 6 Zhang H et al., Snapshot computational spectroscopy enabled by deep learning, *Nanophotonics*. 13, 22 (2024). <https://doi.org/10.1515/nanoph-2024-0328>.
- 7 Doval A, Arosa Y, de la Fuente R, Coupled surface plasmons and resonant optical tunnelling in symmetric optical microcavities, *Opt. Laser Technol.* 192, B (2025). <https://doi.org/10.1016/j.optlastec.2025.113602>.
- 8 Balili RB, Transfer matrix method in nanophotonics, *Int. J. Mod. Phys. Conf. Ser.* 17 (2012). <https://doi.org/10.1142/S2010194512008057>.
- 9 Kalkal Y, Kumar V, Understanding energy propagation during reflection of an evanescent electromagnetic wave, *Am. J. Phys.* 89, 9 (2021). <https://doi.org/10.1119/1.0004834>.